Magnetic anomaly due to elliptic cylinder in the uniform exciting field

M. Hvoždara, A. Kaplíková
Geophysical Institute of the Slovak Academy of Sciences[1]

Abstract: The paper presents exact calculation of magnetic field anomaly induced by the uniform geomagnetic field in the presence of two dimensional body with elliptic cross-section. The solution is performed by means of separation of variables in Laplace equation, using orthogonal elliptic cylindrical co-ordinates. The angle between main axis of generating ellipse and inducing field is general. The calculations of ΔT and inclination anomaly are presented for two important cases: i) magnetic cylinder embedded in non magnetic medium, ii) non magnetic elliptic cylinder hollow (e.g. gallery) embedded in unbounded magnetic medium. The comparison of results (profile curves $\Delta T, \Delta I$) calculated by means of derived analytical formulae and those calculated by means of the boundary integral method used in our previous papers is presented also. Their coincidence is good, namely in the region where the anomalies are most pronounced.

Key words: magnetometric models, elliptic cylinder co-ordinates, magnetometric profile measurements, boundary integral methods

1. Introduction

The exact calculation of the magnetic anomalies by means of analytical methods represents till now theoretical basis of geophysical magnetometry. The two-dimensional perturbing body with general elliptic cross-section covers a variety of interesting approximations of geological bodies, having e.g. almost circular surfaces, or narrow elongated ore veins. Some interesting theoretical results for ribbons can be found in e.g. *(Grant and West, 1965)* or *(Logachev and Zacharov, 1979)*, but theoretical formulae are incomplete or omitted. The exact solution for similar dielectric problem by means of conformal mapping in complex variable plane can be found in *(Smythe, 1950)*.

[1] Dúbravská 9, 845 28 Bratislava 45, Slovak Republic; e-mail: geofhvoz@savba.sk

In our paper we present the exact solution of this magnetic induction problem using the Fourier method of separation of variables in the orthogonal elliptic-cylinder co-ordinate system. The obtained exact solution can be used for various bodies of concern in applied magnetometric methods.

2. Formulation of the magnetic potential problem

Let us consider an unbounded space "1" of uniform magnetic permeability μ_1, in which there is situated a two-dimensional cylinder of constant elliptic cross-section and permeability μ_2. The axis of the cylinder coincides with the y-axis, so the x, z plane intersects it in the ellipse with semiaxes a, b, as shown in Fig. 1. The angle between inducing field $\boldsymbol{B}_0$ (in nT) and

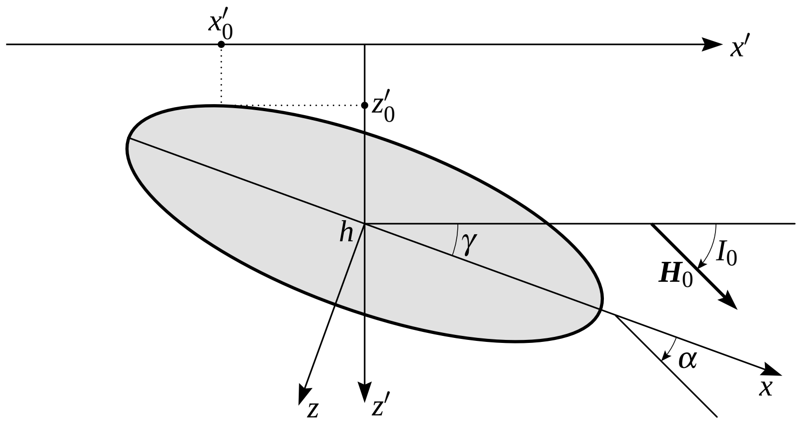

Fig. 1. Geometrical parameters of the magnetic body with elliptic cross-section.

axis x is denoted as α, so the potential for the intensity of the unperturbed field is:

$$U_0(x, z) = -H_0(x \cos\alpha + z \sin\alpha), \tag{1}$$

where $H_0 = \mu_1^{-1} B_0$. Due to the presence of the magnetic body "2" the potential outside is $U_1(x, z)$ and inside $U_2(x, z)$, both are different from (1) their perturbing parts being denoted by the asterics: U_1, U_2, respectively. Then we have potentials in regions "1" and "2":

$$U_1(x,z) = U_0(x,z) + U_1^*(x,z), \tag{2}$$

$$U_2(x,z) = U_0(x,z) + U_2^*(x,z). \tag{3}$$

Since the magnetic field is static, its intensity $\boldsymbol{H}$ is calculated by means of $\operatorname{grad} U$:

$$\boldsymbol{H}_{1,2} = -\operatorname{grad} U_{1,2}(x,z), \tag{4}$$

and magnetic induction $\boldsymbol{B}$:

$$\boldsymbol{B}_{1,2} = \mu_{1,2} \cdot \boldsymbol{H}_{1,2}. \tag{5}$$

From the Maxwell equation we know that $\operatorname{div} \boldsymbol{H} = 0$, so potentials $U_{1,2}$ obey Laplace equations:

$$\nabla^2 U_{1,2} = 0. \tag{6}$$

The potential $U_0(x,z)$ of the uniform magnetic intensity given (1) satisfies the Laplace equation automatically, the perturbing potentials $U_{1,2}^*$ must obey it too:

$$\nabla^2 U_{1,2}^*(x,z) = 0. \tag{7}$$

It is clear, that for infinite distant points $P(x,z)$ from the cylinder, we must have zero limit of U_1^*:

$$\lim_{P\to\infty} U_1^*(x,z) = 0. \tag{8}$$

On the boundary L of the cylinder we must have continuous transition of potentials $U_{1,2}$ and continuous transition of normal component of $\boldsymbol{B}$, which is equal $\mu \partial U/\partial n$.

3. Calculation of the boundary value problem in the elliptic cylinder co-ordinates

We shall transform the Carthesian (x,z) co-ordinates into elliptic-cylinder curve linear co-ordinates (ξ,η) using slightly modified formulae from *Angot (1957)*:

$$x = c \operatorname{ch}\xi \cos\eta, \quad z = c \operatorname{sh}\xi \sin\eta,$$

$$\xi \in \langle 0, +\infty), \quad \eta \in \langle 0, 2\pi\rangle. \tag{9}$$

The Lamé's metrical coefficients are:

$$h_\xi = h_\eta = c(\operatorname{sh}^2\xi + \sin^2\eta)^{1/2} = c(\operatorname{ch}^2\xi - \cos^2\eta)^{1/2}, \tag{10}$$

where c is the geometrical parameter of transformation. The Laplace equation for the potential $U(\xi, \eta)$ is simple:

$$\frac{\partial^2 U}{\partial \xi^2} + \frac{\partial^2 U}{\partial \eta^2} = 0, \tag{11}$$

where we have omitted the multiplicative factor $(h_\xi h_\eta)^{-1}$.

The advantage of co-ordinates (ξ, η) lies in the property that the circumference of the ellipse is the co-ordinate line $\xi = \xi_0$, which follows from (9):

$$x = c\operatorname{ch}\xi_0\cos\eta, \quad z = c\operatorname{sh}\xi_0\sin\eta.$$

Then we have the canonical equation of the ellipse:

$$\frac{x^2}{[c(\operatorname{ch}\xi_0)]^2} + \frac{z^2}{[c(\operatorname{sh}\xi_0)]^2} = 1. \tag{12}$$

Now we match the lengths of semiaxes a, b:

$$a = c\operatorname{ch}\xi_0, \quad b = c\operatorname{sh}\xi_0, \tag{13}$$

which gives important relations:

$$c = \sqrt{a^2 - b^2}, \tag{14}$$

$$\mathrm{e}^{\xi_0} = (a + b)/c, \quad \mathrm{e}^{-\xi_0} = (a - b)/c. \tag{15}$$

The region "1" is now $\xi > \xi_0$, and "2" is $\xi < \xi_0$. These relations match the co-ordinate system (ξ, η) to our case of elliptical contour. The unperturbed potential (1) is expressed in $(\xi\eta)$ variables in the following formula:

$$U_0(\xi, \eta) = -H_0 c[\operatorname{ch}\xi\cos\eta\cos\alpha + \operatorname{sh}\xi\sin\alpha\sin\eta]. \tag{16}$$

One can easily find that the particular solution of the Laplace equation (11) for $U(\xi, \eta)$ is:

$$U_n(\xi, \eta) = \begin{Bmatrix} \mathrm{e}^{n\xi} \\ \mathrm{e}^{-n\xi} \end{Bmatrix} \begin{Bmatrix} \cos n\eta \\ \sin n\eta \end{Bmatrix}, \quad n = 0, 1, 2, \ldots \tag{17}$$

Since in unperturbed potential (16) we have the dependence on η via $\cos\eta$ and $\sin\eta$, we can show that from particular solution (17) we must use only terms for $n = 1$ i.e.:

$$U^*(\xi,\eta) = \begin{Bmatrix} e^{\xi} \\ e^{-\xi} \end{Bmatrix} \begin{Bmatrix} \cos\eta \\ \sin\eta \end{Bmatrix} . \tag{18}$$

The perturbing potential outside the cylinder is:

$$U_1^*(\xi,\eta) = -H_0\, c\, e^{-\xi}[C_1\cos\eta + F_1\sin\eta]. \tag{19}$$

The perturbing potential inside the cylinder $\xi < \xi_0$ is found in the form:

$$U_2^*(\xi,\eta) = -H_0\, c[A_1 \operatorname{ch}\xi\cos\eta + E_1 \operatorname{sh}\xi \sin\eta]. \tag{20}$$

The selection of $\operatorname{ch}\xi$ and $\operatorname{sh}\xi$ will ensure the continuity of both components in $\operatorname{grad} U_2^*$ on the x axis ($x \in \langle -a, +a\rangle$), which is identical with $\xi = 0$ and $\eta = 0$ or $\eta = \pi$. On the surface of the cylinder we must use the boundary conditions:

$$[U_1]_{\xi=\xi_0} = [U_2]_{\xi=\xi_0}\,, \tag{21}$$

$$[\partial U_1/\partial\xi]_{\xi=\xi_0} = \mu_r\,[\partial U_2/\partial\xi]_{\xi=\xi_0}\,, \tag{22}$$

where

$$\mu_r = \mu_2/\mu_1 = (1+\kappa_2)/(1+\kappa_1), \tag{23}$$

where κ_1, κ_2 is magnetic susceptibility of "1" or "2". Using these conditions we obtain a system of two equations for cosine coefficients:

$$-\,e^{-\xi_0}\;C_1 = -A_1\operatorname{ch}\xi_0,$$

$$-\operatorname{sh}\xi_0\cos\alpha + e^{-\xi_0}\,C_1 = -\mu_r\operatorname{sh}\xi_0\cos\alpha - \mu_r A_1\operatorname{sh}\xi_0.$$

The solution is:

$$A_1 = \frac{(1-\mu_r)b\cos\alpha}{a + b\mu_r}, \tag{24}$$

$$C_1 = A_1\, e^{\xi_0}\operatorname{ch}\xi_0 = e^{\xi_0}\left(\frac{a}{c}\right)\frac{(1-\mu_r)}{a+b\mu_r} b\cos\alpha, \tag{25}$$

where we have used relations (13). For coefficients at $\sin\eta$ we have similar equations:

$$F_1\,\mathrm{e}^{-\xi_0} = E_1 \,\mathrm{sh}\,\xi_0,$$

$$-\,\mathrm{ch}\,\xi_0 \sin\alpha + F_1\,\mathrm{e}^{-\xi_0} = -\mu_r\,\mathrm{ch}\,\xi_0 \sin\alpha - \mu_r E_1\,\mathrm{ch}\,\xi_0 .$$

The solution gives:

$$E_1 = \frac{1-\mu_r}{b+a\mu_r} a\sin\alpha, \tag{26}$$

$$F_1 = E_1 (b/c)\,\mathrm{e}^{\xi_0} . \tag{27}$$

In this manner we know the necessary coefficients for the perturbing potentials. The total potential inside the cylinder is expressed clearly in x, z variables:

$$\begin{aligned} U_2(x,z) &= U_0(x,z) + U_2^*(x,z) = -H_0(x\cos\alpha + z\sin\alpha) - \\ &\quad - H_0(1-\mu_r)\left[\frac{b}{a+b\mu_r} x\cos\alpha + \frac{a}{b+a\mu_r} z\sin\alpha\right] = \\ &= -H_0\left\{\left[1+\frac{(1-\mu_r)b}{a+b\mu_r}\right] x\cos\alpha + \left[1+\frac{(1-\mu_r)a}{b+a\mu_r}\right] z\sin\alpha\right\}. \end{aligned} \tag{28}$$

The Carthesian components of the $\boldsymbol{H}_2$ field are equal to $-\,\mathrm{grad}\,U_2$:

$$H_{2x} = H_0 \frac{a+b}{a+b\mu_r}\cos\alpha, \quad H_{2z} = H_0 \frac{a+b}{b+a\mu_r}\sin\alpha. \tag{29}$$

We can see an interesting result, that the magnetic intensity inside the cylinder is a uniform vector field, but its inclination angle is β, generally different from α, as shown in:

$$\mathrm{tg}\,\beta = H_{2z}/H_{2x} = \frac{a+b\mu_r}{b+a\mu_r}\,\mathrm{tg}\,\alpha. \tag{30}$$

This property was often in magnetometry qualitatively quoted, but without explicit formula. Let us introduce a factor of modification of angle α into β:

$$Q_\alpha(v) = \frac{a + b\mu_r}{b + a\mu_r} = \frac{1 + v\mu_r}{v + \mu_r}, \tag{31}$$

where $v = b/a$ characterizes "ellipticity". We can easily find its limit properties:

$$\lim_{v\to 1} Q_\alpha(v) = 1,$$

which is the case of circular cylinder, in which the isolines preserve inclination angle α. Similarly we have

$$\lim_{v\to 0} Q_\alpha(v) = 1/\mu_r,$$

which is the case of thin magnetic strip in the interval $x \in (-a, +a)$, having permeability μ_r. In Figs. 2a,b there are plotted values of $Q_\alpha(v)$ for $v \in \langle 0, 1\rangle$ and various μ_r in the interval $\langle 0.9, 1.1\rangle$. The curves in Fig. 2b show values of β for the outer field inclination $\alpha = 75°$. Using these curves, we can determine the direction of the magnetic line forces inside the cylinder. The intensity component of this uniform magnetic field can be calculated from (29). The perturbing potential outside the cylinder can be expressed by as:

$$U_1^*(\xi,\eta) = -H_0(1-\mu_r)ab\,\mathrm{e}^{-(\xi-\xi_0)}\cdot\left[\frac{\cos\alpha\cos\eta}{a+b\mu_r} + \frac{\sin\alpha\sin\eta}{b+a\mu_r}\right], \tag{32}$$

which shows that it is zero at $\mu_r = 1$ (no magnetic contrast of the cylinder). This formula can be easily derived with respect to ξ or η, which enables us to calculate the curvilinear components of the intensity $\boldsymbol{H}_1^*$:

$$H_{1\xi}^* = -\frac{1}{h_\xi}\frac{\partial U_1^*}{\partial\xi}, \quad H_{1\eta}^* = -\frac{1}{h_\eta}\frac{\partial U_1^*}{\partial\eta}, \tag{33}$$

where

$$h_\xi = h_\eta = c\left[\mathrm{ch}^2\,\xi - \cos^2\eta\right]^{1/2} \tag{34}$$

are Lame's coefficients. The Carthesian components H_{1x}^*, H_{1z}^* are obtained using the formulae of transformation vector components between curvilinear (ξ,η) and Carthesian co-ordinate systems *(e.g. Angot, 1957).*

$$H_{1x}^* = -\frac{c}{h_\xi^2}\left[\frac{\partial U_1^*}{\partial\xi}\,\mathrm{sh}\,\xi\cos\eta - \frac{\partial U_1^*}{\partial\eta}\,\mathrm{ch}\,\xi\sin\eta\right],$$

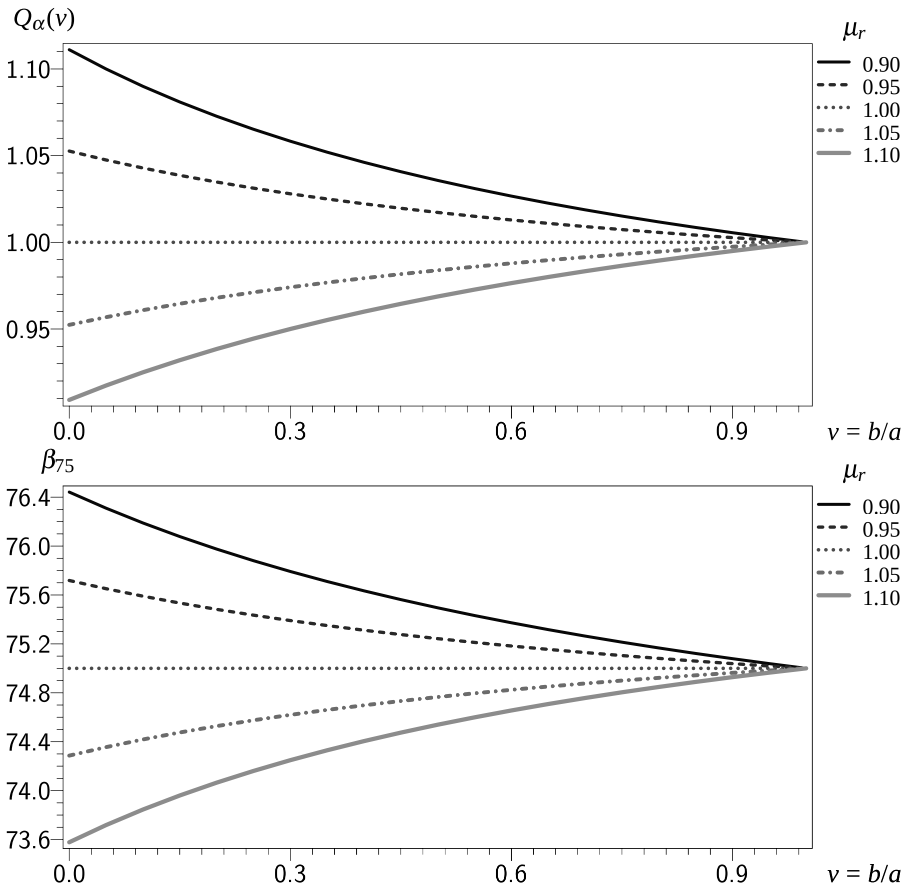

Fig. 2. Modification factor $Q_\alpha(v)$ for various permeabilities μ_r (top panel) and calculated angle β = inclination of the magnetic field inside the cylinder for $\alpha = 75^\circ$ (inclination of outer field with respect to the main axis of the ellipse) – bottom panel.

$$H^*_{1z} = -\frac{c}{h^2_\xi}\left[\frac{\partial U^*_1}{\partial \xi}\operatorname{ch}\xi\sin\eta + \frac{\partial U^*_1}{\partial \eta}\operatorname{sh}\xi\cos\eta\right]. \tag{35}$$

For completeness we must also give formulae for calculating co-ordinate system (ξ, η) from (x, z). For this purpose we use the known property of points (x, z) on the ellipse with semiaxes A, B:

$$\frac{x^2}{A^2} + \frac{z^2}{B^2} = 1. \tag{36}$$

On the other hand, using transformation formulae (9),

$$\frac{x^2}{c^2 \operatorname{ch}^2 \xi} + \frac{z^2}{c^2 \operatorname{sh}^2 \xi} = 1, \tag{37}$$

which gives for pertinent constant the co-ordinate ξ:

$$A = c \operatorname{ch} \xi, \quad B = c \operatorname{sh} \xi, \tag{38}$$

where $c = \sqrt{a^2 - b^2}$, which matches the entire family of confocal ellipses $\xi =$ const. contours to the basic ellipse ξ_0. From the geometrical definition of the ellipse points (x, z) we know, that the sum of their distances from the foci at points $x = \pm c$ is constant and equals to $2A$, i.e.

$$2A = \sqrt{(x-c)^2 + z^2} + \sqrt{(x+c)^2 + z^2} = 2c \operatorname{ch} \xi. \tag{39}$$

Using relation $\operatorname{sh} \xi = \sqrt{\operatorname{ch}^2 \xi - 1} = B/c$ we obtain

$$\mathrm{e}^{\xi} = (A + B)/c, \quad \mathrm{e}^{-\xi} = (A - B)/c, \tag{40}$$

which enables us to calculate the ξ co-ordinate. The angle co-ordinate η will be determined from relation:

$$\operatorname{tg} \eta = (z/x) \cdot (A/B)\,. \tag{41}$$

It is clear that $\eta = 0$ for $z = 0$ and $x > 0$, $\eta = \pi$ for $z = 0$ and $x < 0$. Along the axis $z > 0$ we have $\eta = \pi/2$. In this manner we can use the calculation of (ξ, η) co-ordinates for required network of points (x, z).

4. Numerical calculation for some models

For the geophysical purposes we must generalize the derived formulae for the case when the axis of the cylinder is buried at some depth h and the main axis is inclined by the angle $\gamma \in (0, \pi/2\rangle$ with respect to the surface plane, as shows Fig. 1.

The transformation relations are:

$$x = x' \cos\gamma + (z' - h)\sin\gamma, \quad z = -x' \sin\gamma + (z' - h)\cos\gamma. \tag{42}$$

These (x, z) must be used for calculations of (ξ, η). If the angle of inclination of unperturbed field with respect to the x' axis is I_0, we have to put into previous formulae

$$\alpha = I_0 - \gamma. \tag{43}$$

In this manner we can link the "elliptic formulae" to the more general co-ordinate system. It is also interesting to determine the co-ordinates (x'_0, z'_0) which correspond to the point nearest to the surface. Using the formulae of analytical geometry in the (x, z) variables we have:

$$x = a\cos\varphi, \quad z = b\sin\varphi,$$

where the angle φ is reckoned from the x axis. Using transformation (42) we obtain:

$$z' = h + a\sin\gamma\cos\varphi + b\cos\gamma\sin\varphi. \tag{44}$$

The extremum of the value z' with respect to φ is determined using condition $\partial z'/\partial\varphi = 0$, and for the value φ_0 we have:

$$\operatorname{tg}\varphi_0 = (b\cos\gamma)/(a\sin\gamma). \tag{45}$$

Because from the geometrical analysis of Fig. 3 there must be $\pi \leq \varphi_0 \leq \frac{3}{2}\pi$, thus:

$$\sin\varphi_0 = -(b/p)\cos\gamma, \quad \cos\varphi_0 = -(a/p)\sin\gamma, \tag{46}$$

where $p = \left[b^2\cos^2\gamma + a^2\sin^2\gamma\right]^{1/2}$. Substitution of $\cos\varphi_0$ and $\sin\varphi_0$ into (44) gives minimum of z' for the circumference of the ellipse:

$$z'_0 = h - \left[a^2\sin^2\gamma + b^2\cos^2\gamma\right]^{1/2} = h - p. \tag{47}$$

Similarly we obtain for the horizontal co-ordinate of the minimum:

$$x'_0 = \left[(a^2 - p^2)/p\right] \cdot \operatorname{tg}\gamma. \tag{48}$$

The FORTRAN 90 program of our computations was designed for the calculation of $\Delta T, \Delta I, \Delta Z$ along x' profiles running at various levels of z' above the cylinder. If we calculate the components of anomalous field: (H^*_{1x}, H^*_{1z}) in co-ordinate system (x, z), we transform these components into "measuring" co-ordinate system (x', z') using relations:

$$H^*_{1x'} = H^*_{1x} \cos\gamma - H^*_{1z} \sin\gamma, \quad H^*_{1z'} = H^*_{1x} \sin\gamma + H^*_{1z} \cos\gamma. \tag{49}$$

The most interesting characteristics of the geomagnetic anomaly are the anomaly of total field (ΔT) and the anomaly of inclination ΔI. These are calculated as follows:

$$\Delta T = \mu_0 \left[(H_{0x'} + H^*_{1x'})^2 + (H_{0z'} + H^*_{1z'})^2\right]^{1/2} - \\ - \mu_0 \left[(H^2_{0x'} + H^2_{0z'})\right]^{1/2}, \tag{50}$$

$$\Delta I = \mathrm{arctg}\left[(H_{0z'} + H^*_{1z'})/(H_{0x'} + H^*_{1x'})\right] - I_0. \tag{51}$$

Here $H_{0x'}, H_{0z'}$ denote the horizontal and vertical components of the unperturbed geomagnetic field intensity corresponding to $\boldsymbol{B}_0$.

For numerical calculations we chose an elliptic cylinder with semiaxes $a = 10\,\mathrm{m}$, $b = 5\,\mathrm{m}$ and slope angle $\gamma = 0°$ or $\gamma = 30°$. The relative permeability $\mu_r = 1.1$ corresponds to the magnetic ore body and $\mu_r = 0.9$ corresponds to the case of non-magnetic cavity (gallery) $\mu_2 = \mu_0$, which is excavated in the weakly magnetic space $\mu_1 = \mu_0(1 + \kappa_1)$ of susceptibility $\kappa_1 = 0.1111 = 1/9$. The value of normal field was taken as $B_0 = 47000\,\mathrm{nT}$, its inclination $I_0 = 75°$. The vector $\boldsymbol{B}_0$ was supposed perpendicular to the strike axis y of the cylinder. In Figs. 3a,b we can see the curves of ΔT and ΔI along x' profiles above the elliptic cylinder at the depths $z'/d = -0.6$, -0.3, 0, 0.3, 0.6. The anomalies are weak far from the body $z'/d = -0.6$, -0.3 and increase when the observation profile approaches to the top of the body (the length norm d put $d = a$). The maxima of ΔT occur at $x'/d \approx -0.5$, minima in the far zone $x'/d > 1$. It is interesting that the inclination anomalies obtain values of few tens of angle minutes.

The effect of non-magnetic elliptic cylinder cavity ($\mu_r = 0.9$) can be seen in Figs. 4a,b. The course of curves ΔT and ΔI is approximately of negative values in comparison to the magnetic case presented in Figs. 3a,b.

It is interesting also to compare the presented "analytical" results for the elliptic cylinder with results obtained by the boundary integral method

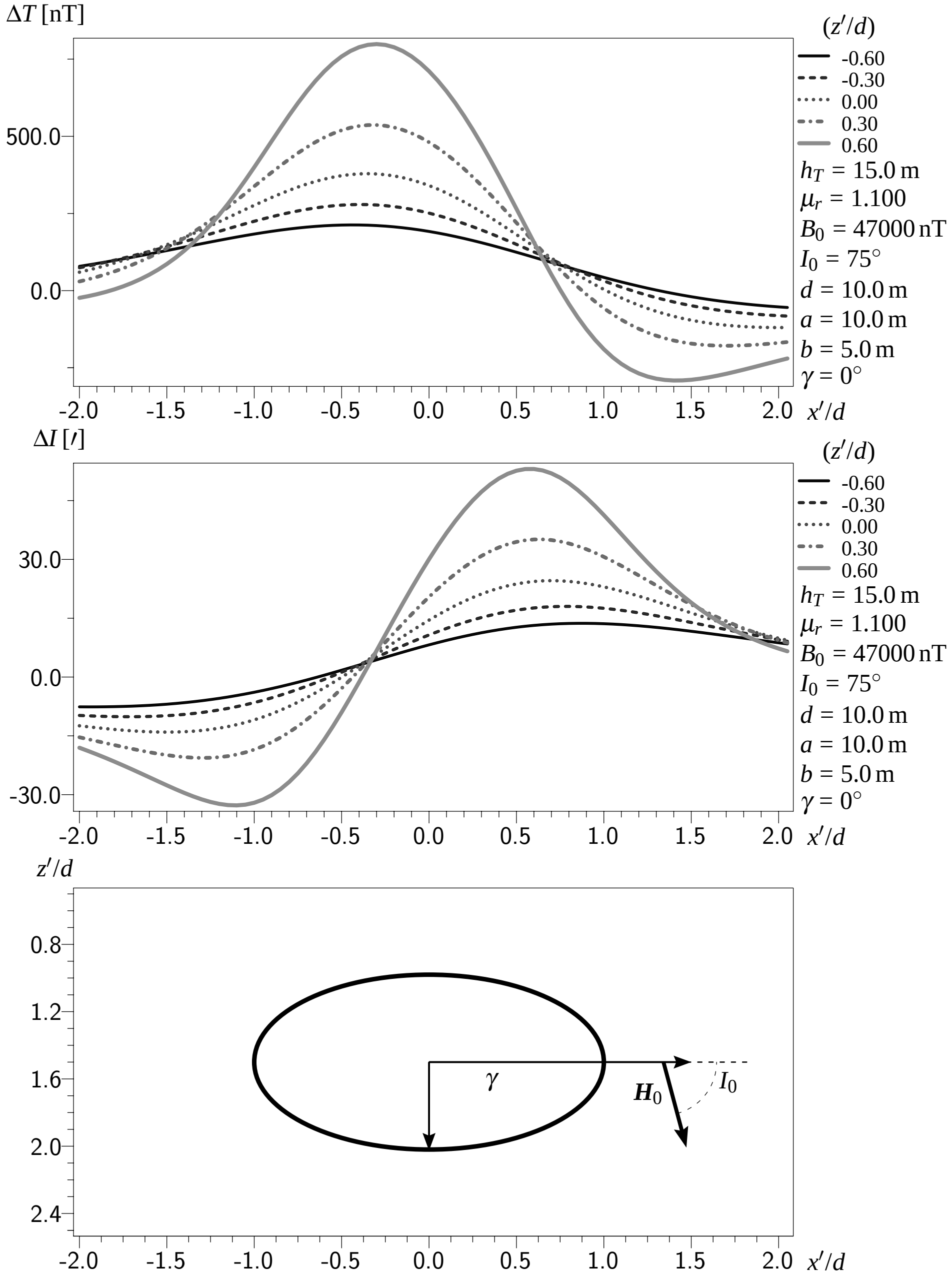

Fig. 3a. Profile curves of ΔT and ΔI for magnetic elliptic cylinder, $\gamma = 0^{\circ}$.

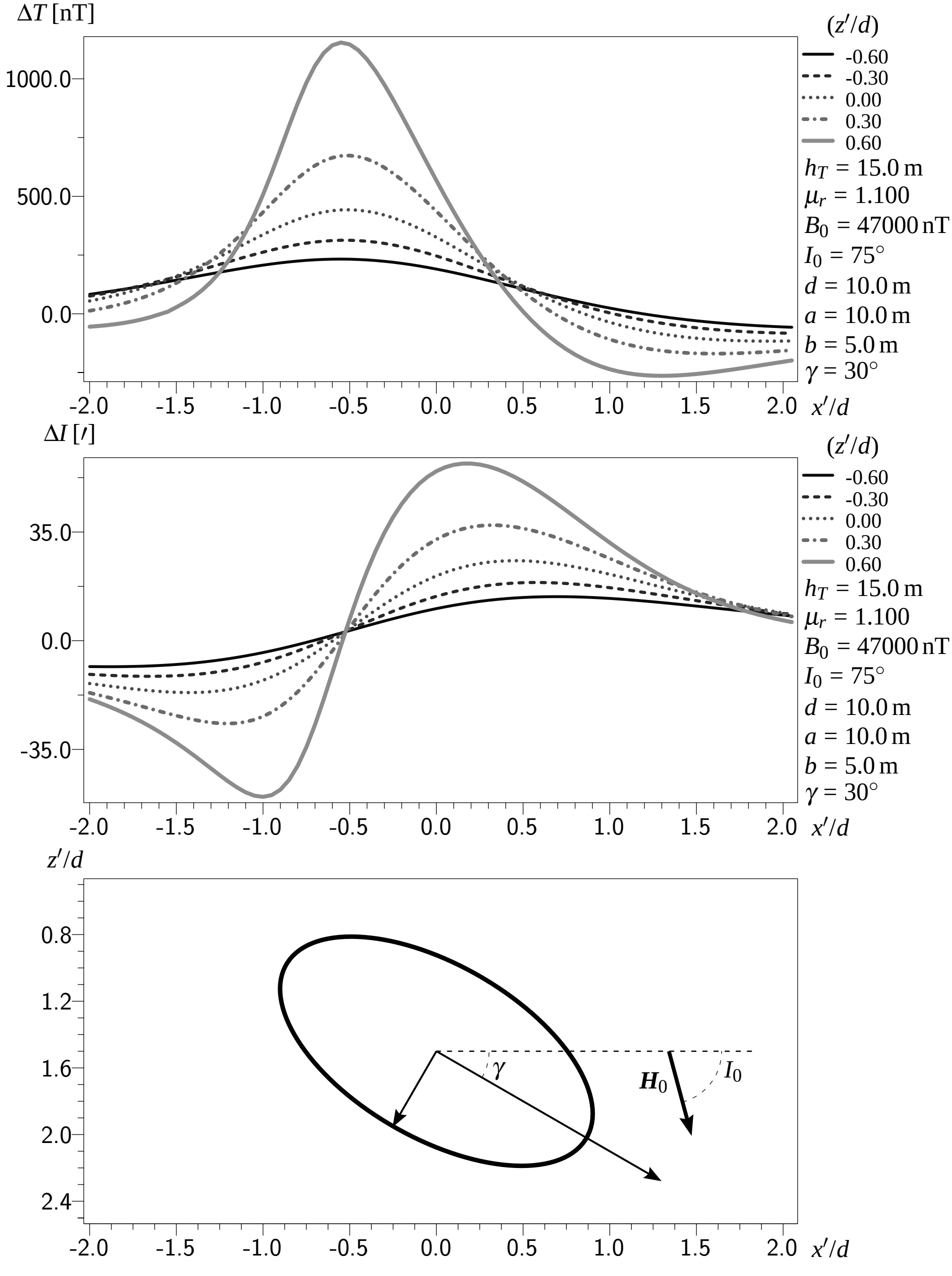

Fig. 3b. Profile curves of ΔT and ΔI for magnetic elliptic cylinder, $\gamma = 30°$.

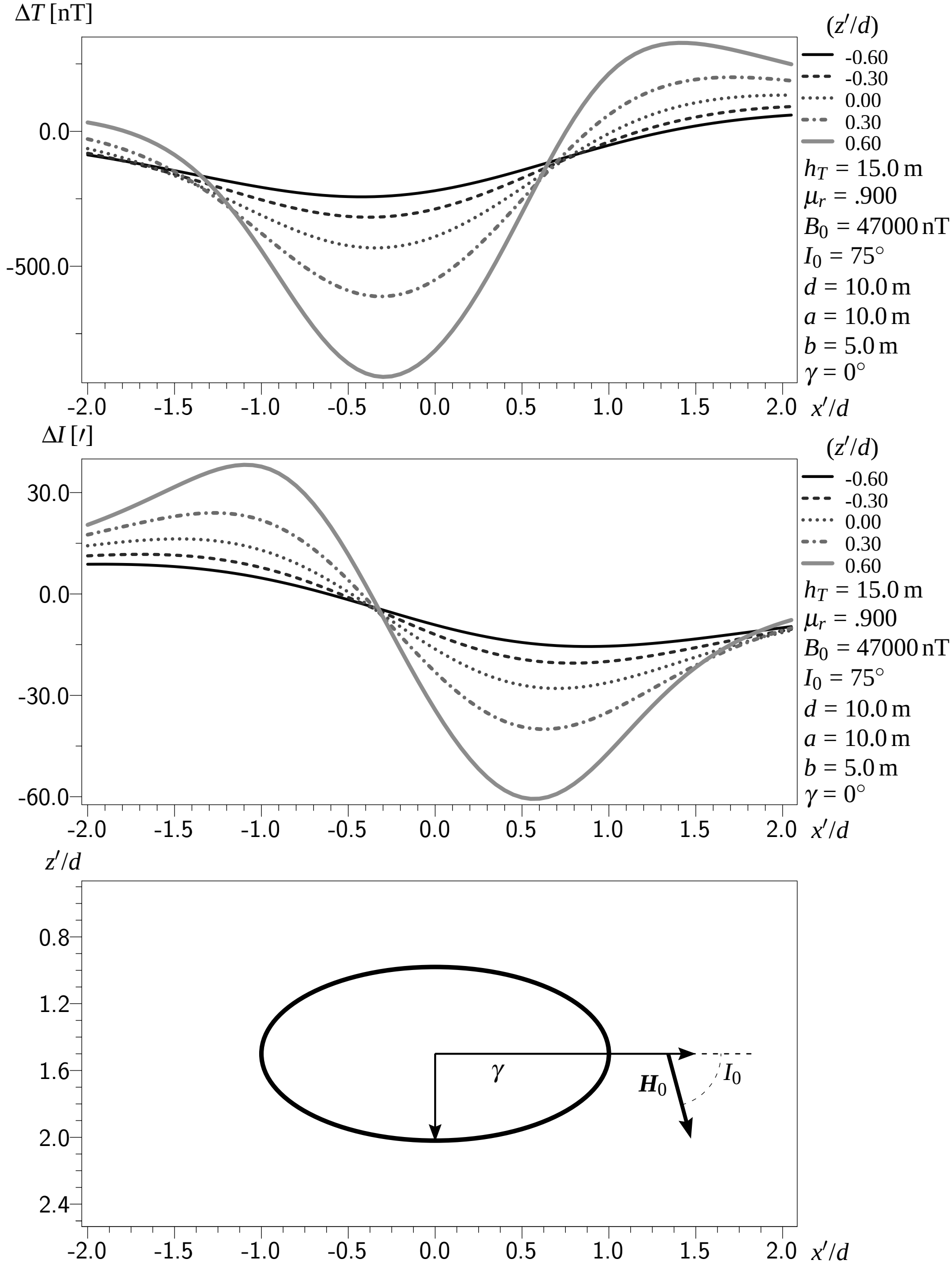

Fig. 4a. Profile curves of ΔT and ΔI for non-magnetic elliptic cylinder, $\gamma = 0^\circ$.

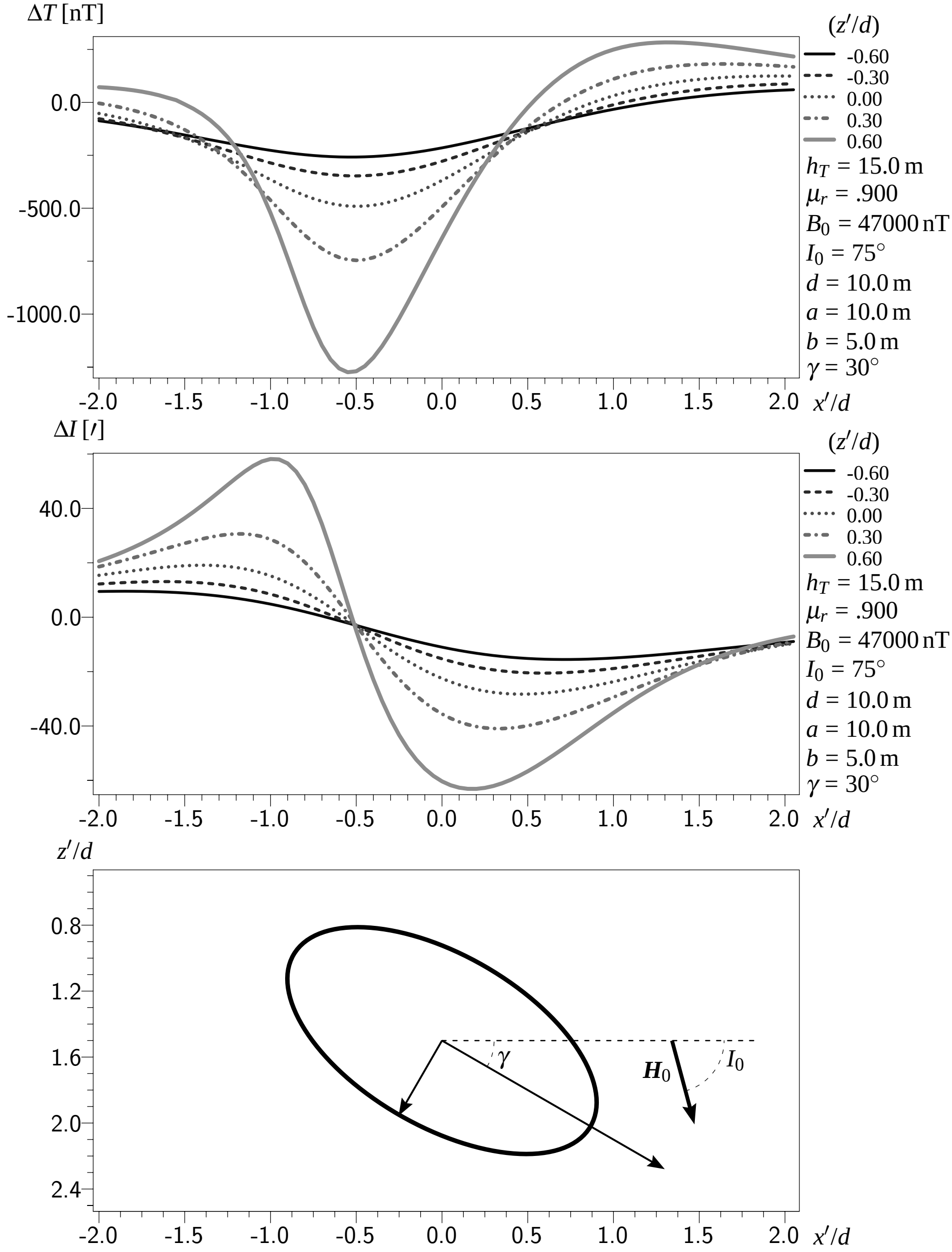

Fig. 4b. Profile curves of ΔT and ΔI for non-magnetic elliptic cylinder, $\gamma = 30^\circ$.

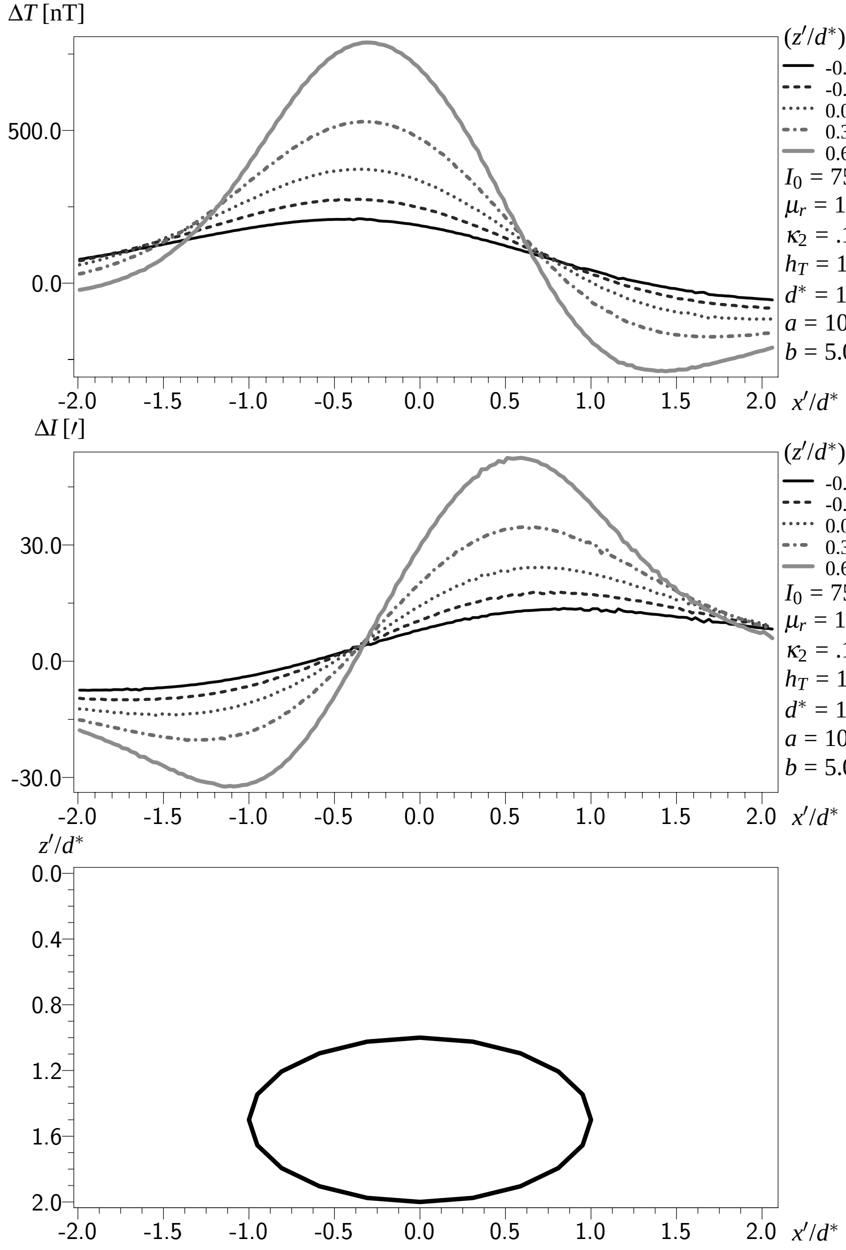

Fig. 5a. Profile curves of ΔT and ΔI for magnetic elliptic cylinder, $\gamma = 0^\circ$ – calculated by boundary integral method.

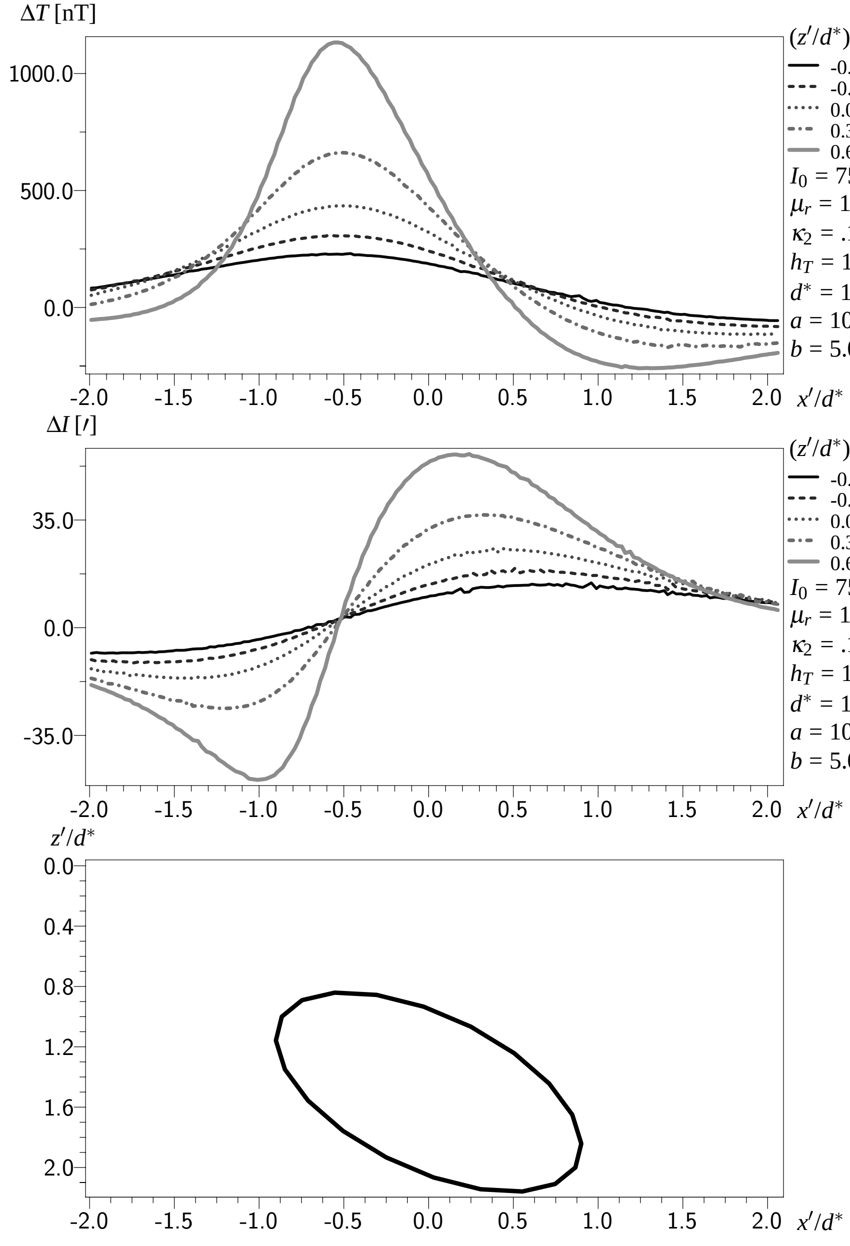

Fig. 5b. Profile curves of ΔT and ΔI for magnetic elliptic cylinder, $\gamma = 30^\circ$ – calculated by boundary integral method.

(BIM) presented in *(Hvoždara and Kaplíková, 2005)*. For this purpose we approximated the elliptic contour by the equilateral polygon with 20 vertices. In Figs. 5a,b we present results from the BIM approximation of the elliptic cylinder with parameters corresponding to Figs. 3a,b. We can see that the profile curves ΔT, ΔI match very well. There occurs only a small ripple at the points very distant from the axis of the cylinder. This is caused by using approximation of the anomalous field components as finite differences of anomalous potential. From the practical point of view we can accept the BIM algorithm as well confirmed, and use it for more general anomalous magnetic bodies with irregular cross-sections.

Acknowledgments. The authors are grateful to the Slovak Grant Agency VEGA (grant No. 2/4042/24) for the partial support of this work.

References

Angot A., 1957: Complement de mathematiques, Paris (Czech translation: Angot A.: Užitá matematika pro elektrotechnické inženýry. SNTL Praha 1960).

Grant F. S., West G. F., 1965: Interpretation Theory in Applied Geophysics. McGraw-Hill Book Comp., New York.

Hvoždara M., Kaplíková A., 2005: Magnetometric problem for a 2-D body of polygonal cross-section buried in the unbounded magnetic halfspace. Contr. Geophys. Geod., **35**, 4, 353–372.

Logachev A. A., Zacharov V. P., 1979: Magnetometry. Nedra, Leningrad (in Russian).

Smythe W. R., 1950: Static and dynamic electricity. McGraw-Hill Book Comp., New York.